ISSN 2176-5480

22nd International Congress of Mechanical Engineering (COBEM 2013)
November 3-7, 2013, Ribeirão Preto, SP, Brazil

PITCH CONTROL OF ROBOTIC VEHICLES DURING BALLISTIC MOTION

Pedro Ferreira da Costa Blois de Assis, prblois@gmail.com
Marco Antonio Meggiolaro, meggi@puc-rio.br
Pontifical Catholic University of Rio de Janeiro, Department of Mechanical Engineering
Rua Marquês de São Vicente 225, Gávea. Rio de Janeiro, RJ – 22543-900
prblois@gmail.com
meggi@puc-rio.br

Abstract. *Stability control is a known technique used to increase safety in passenger vehicles. Other trends in the automobile industry are electric vehicles with independently driven wheels. Their zero-emitting qualities have made them environmentally attractive and, due to their drivetrain, they tend to be mechanically less complex. Although stability controls work to prevent the vehicle from reaching unstable situations, high speed vehicles hitting obstacles may lose contact with the ground. In these situations, none of the existing stability controls can guarantee safe landing during ballistic motion. This work presents an algorithm for flying wheel detection to help identify ballistic motion and therefore determine the appropriate action to increase the odds of a safe landing. Current sensors and encoders are used by the algorithm. A reaction wheel based control is proposed to stabilize and adjust the pitch angle during ballistic motion to a better landing position. The flying wheel detection algorithm can also estimate external torques acting on the wheel using the same sensors already installed in the motor for current control, making it a costless technique. The detection algorithm and pitch control algorithm presented were tested in a simulator developed for the research. A maximum time of 0.3s for convergence of the pitch angle is guaranteed without saturation of the motors if the initial conditions of angular velocity and orientation obey the linear relationship presented. The results show the potential of the presented algorithms on experimental implementations.*

Keywords: *Attitude control; robotic vehicles; ballistic motion; torque estimation.*

1. INTRODUCTION

Following world tendencies of zero-emitting pollution, the production of hybrid and all-electric vehicles is increasing. One estimates that the number of electric vehicles already on the streets has increased from 50000 in 2011 to 180000 in 2012. The majority of them are found in developed countries like USA, Japan and European countries. China and India also present significant concentrations of electric cars in the streets (IEA - International Energy Agency).

All-wheel driven electric cars with independent motors for each wheel (like the Mercedes SLS AMG Electric Drive) have a less complex drivetrain witch increases the reliability and longevity of the equipment and decreases the losses in the systems. Due to this simplicity the torque is directly applied to the wheels which facilitate the development of control algorithms (Hori, et al., 1997). Systems in the safety area like Anti-locking Braking System and Electronic Stability Systems are some examples.

One of the biggest obstacles for cheaper electric cars is the battery. The main technology used nowadays is the lithium-ion battery. New technologies in the field of batteries are continuously decreasing those costs. Most recently, Phynergy (www.phynergy.com) has been commercializing metal-air batteries with energy density 100 times higher than the conventional lithium-ion ones.

All-electric vehicles with independent motors driving each wheel are common in the fields of robotics. Robotic vehicles can be used for rough terrain exploration such as forests or mines realizing tasks like localization and rescue, inspection of hazardous sites, planet explorations etc.. Due to the roughness of the terrain in some missions, stability control plays an important role for the mission success. Numerous works have been published regarding yaw, roll and pitch dynamic stability for missions where either the velocity is low or the velocity is high but the terrain is smooth (Beal, 2011; Carlson, et al., 2003; Peters, et al., 2011; Rajamani, 2012; Schofield, 2006). (Peters, 2012 and Iagnemma, et al., 2003) have shown significant works for hazardous avoidance during missions in rough terrain at high speeds. In those researches, hazard avoidance has been performed either by selecting from a set of predetermined paths (i.e. search techniques over small spaces), or by reactive (reflexive) behaviors, which evoke a pre-determined action in response to specific sensor signals.

Although successful experiments have been shown in hazardous avoidance, once the obstacle avoidance is not possible, roll and/or pitch instability is likely to be reached and none of the works nowadays deals with this situation. This work presents some mitigation acts to increase the odds of a safe landing after ballistic motion due to bumps or deep ditches. The algorithm is tested on an all-wheel skid-steer electric driven robotic vehicle and aims to control pitch instability through reaction wheels method used in attitude control of satellites.

ISSN 2176-5480

An algorithm for detection of flying wheels is also presented that uses only current sensors and encoders. Considering that torque control of DC motors usually have these sensors, the proposed algorithm adds no extra costs in the system normally spent in distance sensors or force transducers used for the same purpose.

All of the proposed algorithms were tested in a simulator developed for the research described in (Lima, 2010).

2. STABILITY CONTROL TECHNIQUES

In passenger cars, the first stability control established was the ABS (Anti-Lock Braking System), introduced by Bosch in a 1978 Mercedes-Benz. Still widely used, this system releases the wheel's brake whenever it starts to lock preventing it to fully slide while reducing the vehicle's speed. This action increases the vehicle maneuverability during turns (Rajamani, 2012).

The next step was to develop a control system that monitors the driver's intention and compare it to the vehicle actual behavior. The YSC (Yaw Stability Control) system uses this error to send correction signals to control the actuators of the vehicles. This actuation is often made through ABS systems already installed on the vehicles (Beal, 2011). For this combination (YSC with ABS) different braking signals are sent to each side of the vehicle so that the resulting moment applied to the vehicles chassis corrects the yaw instability. One of its disadvantages is the mandatory braking action on every correction with immediate reflex on longitudinal velocity of the vehicle.

Other two techniques used in YSC are steer-by-wire and active-torque distribution. In steer-by-wire systems the command sent by the driver to the steering wheels is overwritten by the control system while in active-torque distribution, electronic differentials are use to set different torques on each wheel. For vehicles with high center of mass like buses and trucks, rollover becomes a threat. For these purpose, the RSC (Roll Stability Control) was developed using the same actuation systems as the ones described above (Rajamani, 2012).

All of the above described control algorithms relies on good traction forces between tire and terrain. The traction control in passengers cars or robotic vehicles are developed, usually, to optimize the longitudinal slip. The typical shape of the relation between the longitudinal slip and the friction coefficient can be seen in Fig. 1. One can see that the maximum friction coefficient occurs for low values of longitudinal slip.

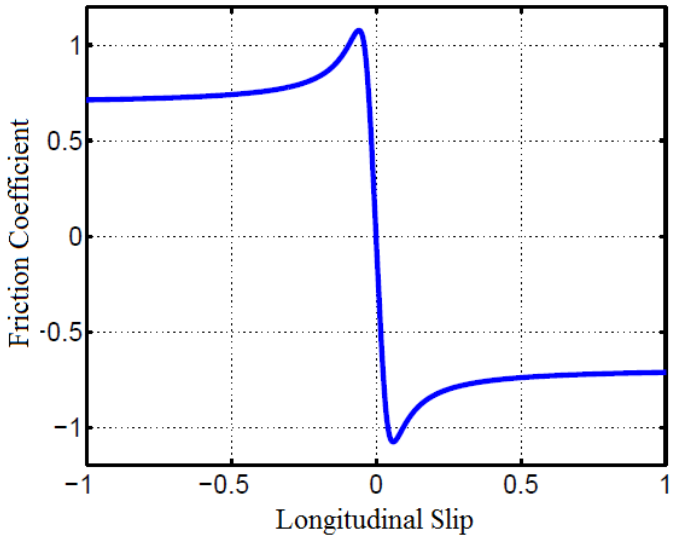

Figure 1. Typical shape of the relation between the friction coefficient and longitudinal slip (Peters, 2012).

However, the forces between tires and terrain are more complex and involves the influence of the sideslip angle of the tire. Peters, et al., (2011) presents a traction control that deals with the non-linearities that arises from the combination of the longitudinal slip with the sideslip angle at high speeds. In (Hori, et al., 1997), a PID controller with a proportional gain varying accordingly with the wheel's spin is presented with good experimental results for traction control. The presented model allows a good estimation of road friction conditions.

Stability control algorithms for the pitch angle have been successfully proposed for robotic vehicles on rough terrain (Silva, 2007; Santos, 2007). The developed algorithms controls the vehicle speed through computed torque control and uses an optimization algorithm to minimize the power dissipated on the motors and maximize the traction force.

Different types of terrains demands different approaches for stability control. Robotic vehicles designed to explore other planets or remote areas of planet Earth should deal with terrain intricacies like loose rocks, holes, swamps etc.. In those scenarios, vehicles tend to be slower and rollover (lateral or longitudinal) becomes a greater concern (Iagnemma, et al., 2004).

ISSN 2176-5480

3. SYSTEM MODELS

Dynamic models of wheeled robots and passengers cars are extensively found in the literature (Beal, 2011; Carlson, et al., 2003; Genta, 1997; Jaza, 2009; Rajamani, 2012; Schofield, 2006). The main model used is the bicycle model where only two wheels are considered: one front steerable wheel and one fixe rear wheel. The longitudinal, lateral and yaw dynamics are considered while neglecting the roll, pitch and vertical dynamics for instabilities analysis. The works that propose rollover stability controllers assume the vehicle as an inverted pendulum with only one degree of freedom. Load transfers between axes are only considered in constant longitudinal or lateral acceleration analysis. For those scenarios the normal forces are different but constant through the entire analysis.

For the flying wheel detection the algorithm uses only the DC motor state model as described below. For the vehicle model used in this paper it is assumed that the vehicle is already in ballistic motion and therefor is considered only the reaction torques acting on the chassis while driving the wheels.

3.1 DC motor model

Direct current motors model is well known and explored in the literature (Ramesh, et al., 2010; Zaccarian). The estimate of the system parameters can be made through step response and any curve fitting method such as Recursive Least Square Method (Krneta, et al., 2005; Salah, 2009).

The robotic vehicle model used in the simulations assumed one dc motor driving each wheel through a gearbox. The differential equations of the motor are shown below.

$$L\frac{di}{dt} = V - Fem - Ri \tag{1}$$

$$J\frac{d\omega_r}{dt} = T_m - b\omega_r - \tau_{ext} \tag{2}$$

$$T_m = K_t G_b i \tag{3}$$

$$Fem = K_t \omega_e \tag{4}$$

where:

- L is the equivalent inductance of the system motor + electronics + battery;
- R is the equivalent resistance of the system motor + electronics + battery;
- i is the electric current through the motor terminals;
- V is the applied voltage;
- J is the equivalent inertia of the system motor + gearbox + wheel;
- b is the equivalent viscous friction constant;
- τ_{ext} is the external torque over the wheel;
- ω_e is the motor's spin;
- ω_r is the wheel's spin;
- G_b is the gearbox ratio;
- K_t is the torque constant.

In the motor used as model for the research (A28-150 Ampflow) the torque constant K_t is equal to the speed constant K_v. The terms Fem e T_m are, respectively, the counter electro-active voltage and the torque after the gearbox (next to the wheel). Due to the gearbox, the wheel's spin is $\omega_r = {}^{\omega_e}/_{G_b}$ changing the Equation 2 to:

$$J\frac{d\omega_e}{dt} = K_t i G_b^2 - b\omega_e - G_b\tau_{ext} \tag{5}$$

The state space model is shown below.

$$\begin{cases} \dot{\boldsymbol{X}}(t) = \underline{A}\boldsymbol{X}(t) + \underline{B}\boldsymbol{U}(t) \\ \boldsymbol{Y}(t) = \underline{C}\boldsymbol{X}(t) \end{cases} \tag{6}$$

where:

ISSN 2176-5480

- $X = \begin{bmatrix} i \\ \omega_e \end{bmatrix}$ is the state vector;
- $\underline{A} = \begin{bmatrix} -R/L & -K_t/L \\ K_t G_b^2/J & -b/J \end{bmatrix}$ is the state matrix;
- $\underline{B} = \begin{bmatrix} 1/L & 0 \\ 0 & -G_b/J \end{bmatrix}$ is the input matrix;
- $\underline{C} = \begin{bmatrix} 1 & 0 \\ 0 & 1 \end{bmatrix}$ is the output matrix;
- Y is the output vector (sensors current meter and encoder);
- $U = \begin{bmatrix} V \\ \tau_{ext} \end{bmatrix}$ is the input vector (applied voltage and external torque).

3.2 Pitch angle dynamic model

Due to the simplicity of the vehicle used as model in this work, the only controllable degree of freedom during ballistic motion is the pitch angle. The dynamic model used is simple and assumes that a moment of inertia is excited by a reaction torque produced by four wheels with no external forces nor internal dissipative efforts. It is also assumed that the angular velocity of the chassis in the other two directions (yaw and roll) is neglected during ballistic motion (which is plausible if the vehicle hits the obstacle with the front wheels at the same time). The model used is $\tau_{tot} = I_c^2 \dot{\omega}_y$, where τ_{tot} is the total torque applied by the four reaction wheels, I_c^2 is the equivalent moment of inertia of the system and $\dot{\omega}_y$ is angular acceleration of the chassis.

4. WHEEL LIFT-OFF DETECTION

In smooth terrains inertial sensors combined with dynamic models of the vehicle can be used to prevent wheel detaching from the ground (Silva, et al., 2010). Nonetheless, high speed vehicles in rough terrain can hit obstacles or ditches and detach one or more wheels from the ground without any warnings from the model predictive. This section presents an algorithm that estimates the external torque over a wheel and determines if this wheel is still in contact with the ground or not.

The algorithm uses the state model of the DC motor presented in section 3.1. Using Zero Order Holder method to discretize the state model from section 3.1 for a control period of *T* seconds, one can reach the following discrete state model shown below.

$$\begin{cases} \boldsymbol{X}_{k+1} = \underline{\Phi}\boldsymbol{X}_k + \underline{\Gamma}\boldsymbol{U}_v \\ \boldsymbol{Y} = \underline{H}\boldsymbol{X}_k \end{cases} \tag{7}$$

where $\underline{\Phi} = e^{AT}$, $\underline{\Gamma} = \underline{B}\int_0^T e^{As} ds$, $\underline{H} = \underline{C}$, $\boldsymbol{X}_k$ is the current state, $\boldsymbol{Y}$ are the sensors readings and $\boldsymbol{U}_v = [V \quad 0]^T$ are the applied voltage and the external torque.

An applied voltage V_0 takes the current state $\boldsymbol{X}_k$ to the next state $\boldsymbol{X}_{k+1}$. If to the same state $\boldsymbol{X}_k$ is applied an external torque τ_{ext} besides V_0, the next state will be $\boldsymbol{X'}_{k+1}$. The difference will be given by the term $\underline{\Gamma}\boldsymbol{U}_\tau$, where $\boldsymbol{U}_\tau = [0 \quad \tau_{ext}]^T$, so that $\boldsymbol{X}'_{k+1} = \underline{\Phi}\boldsymbol{X}_k + \underline{\Gamma}\boldsymbol{U}_v + \underline{\Gamma}\boldsymbol{U}_\tau$. If $\underline{\Gamma}$ is invertible one can estimate the external torque acting on the wheel using the equation below.

$$\boldsymbol{U}_\tau = \underline{\Gamma}^{-1}(\boldsymbol{X}'_{k+1} - \boldsymbol{X}_{k+1}) \tag{8}$$

To determine whether or not the wheel has lost contact with the ground, one can compare $\tau = [0 \quad sign(V)]\boldsymbol{U}_\tau$ with a threshold τ_{lim} chosen accordingly to the noise level of the system. If $\tau > \tau_{lim}$ than an external torque is acting upon the wheel (wheel in contact to the ground), opposing the command given by the applied voltage. If $\tau < \tau_{lim}$ than an external torque is acting upon the wheel (wheel in contact to the ground), aiding the command given by the applied voltage. If $-\tau_{lim} < \tau < \tau_{lim}$ the wheel has lift-off the ground.

Due to noisy sensors, the estimative can oscillate significantly and occasionally enter the lift-off the ground zone without actual lift-off (false-positive detection). To minimize this effect, four stages were created for the algorithm. The first one indicates that all wheels are in contact with the ground. The second stage indicates that the front wheels have detached from the ground. The third stage is a warning stage where all wheels seem to be off the ground but time is needed to verify the information. If the algorithm remains detecting that all wheels are off the ground for more than 0.1 s, then the ballistic motion stage (fourth and last stage) is on.

ISSN 2176-5480

5. PITCH CONTROL

Iagnemma, et al. (2003) presents a stability control algorithm based o reactive behavior where pre-determined actions are consulted from a database during the experiment. The action is chosen based on the obstacle detected. Those actions are calculated offline using the dynamic models developed for the system. The type of behavior is triggered by one or more sensor readings. Although it deals with high speed vehicles on rough terrain, once the wheels are lift-off, nothing can be done but wait.

This section presents an algorithm for correction of the vehicle's pitch angle after wheel's lift-off (during ballistic motion) that aims to increase the odds of a safe landing. The proposed technique for pitch angle correction during ballistic motion is inspired in satellite attitude control through reaction wheels (Nudehi, et al., 2008; Roberts, et al., 2004).

The destabilization of the vehicle can be divided into three categories: lateral destabilization (when two wheels from the same side lift-off the ground); longitudinal destabilization (when either front or back wheels lift-off the ground); and total destabilization (ballistic motion where all wheels are off the ground). This paper deals only with the ballistic motion.

The system to be control is a pure integrator and can be stabilized with a PD controller. The closed loop transfer function of the system is shown below.

$$H(s) = \frac{K_p(T_d s+1)}{I_c s^2+K_p(T_d s+1)} \tag{9}$$

where:

- K_p is the proportional gain of the controller;
- T_d is the derivative gain of the controller;
- I_c is the equivalent moment of inertia of the system.

From (Ogata, 2011), the smallest settling time of a second order system occurs for a damping factor ξ of 0.76 for a 2% tolerance of the final value. The controller is designed to correct the pitch angle in less than 0.3 s. This time considers a minimum height of 1 m for the ballistic motion. Another limitation of the system is the 40 Nm maximum torque available on each wheel.

Assuming that the maximum control signal is commanded instantly as the ballistic motion is detected and that the desired values of pitch angle and velocity are zero, the control law can be determined as:

$$U = K_p\left(T_d \omega_{y0} + \phi_{y0}\right) \tag{10}$$

where:

- ϕ_{y0} is the initial condition for the pitch angle;
- ω_{y0} is the initial condition for the pitch angular velocity;
- U is the control signal.

The choice of a damping factor of 0.76 implies a dependency between the controller gains as shown below.

$$K_p = \frac{0.76^2 4 I_c}{{T_d}^2} \tag{11}$$

Substituting Eq. (11) in Eq. (10) and considering the saturation of the motors, the control law can be determined by the equation below.

$$U = \frac{2{,}31 I_c}{{T_d}^2}\left(\phi_{y0} + T_d \omega_{y0}\right) \leq 160Nm \tag{12}$$

Considering the maximum convergence time of 0.3 s, the controller gains are determined as $T_d \geq 0.17$s and $K_p = 76.3 I_c$. Those values restrict the initial conditions as shown below.

$$\phi_{y0} \leq 160 \frac{{T_d}^2}{2{,}31 I_c} - T_d \omega_{y0} \tag{13}$$

If the initial conditions satisfy Eq. (13), it is guaranteed that the pitch angle and pitch angular velocity will converge to zero in approximate 0.3s without saturating the motors.

ISSN 2176-5480

6. RESULTS

A simulator was developed for this research and more details can be found in (Lima, 2010). The model parameters of the dc motors used in the simulations were taken from the A28-150 Ampflow dc motor and can be seen in the table below.

Table 1: DC motor parameters used in the simulations.

Parameter	**Value**
Resistance	0.148 Ω
Inductance	0.5 mH
Torque Constant ($k_t = k_v$)	0.03757 Vs/rad

The iteration period used during simulations was of 75 μs. The wheels were considered to have inertia of 0.054 kg/m^2 and the gearbox between the wheel and the motor have a ratio of 1:7.14.

The robot simulated was a 58kg skid-steer electric vehicle with four independently driven wheels. The chassis length, width and height are, respectively, 0.64m, 0.22m and 0.10m. The wheels were considered massless due to its direct coupling to the chassis (no suspensions). The parameters were taken from a robotic vehicle used for pipe inspection developed in the Robotic Laboratory of PUC-Rio. The figure below shows a CAD model of the vehicle.

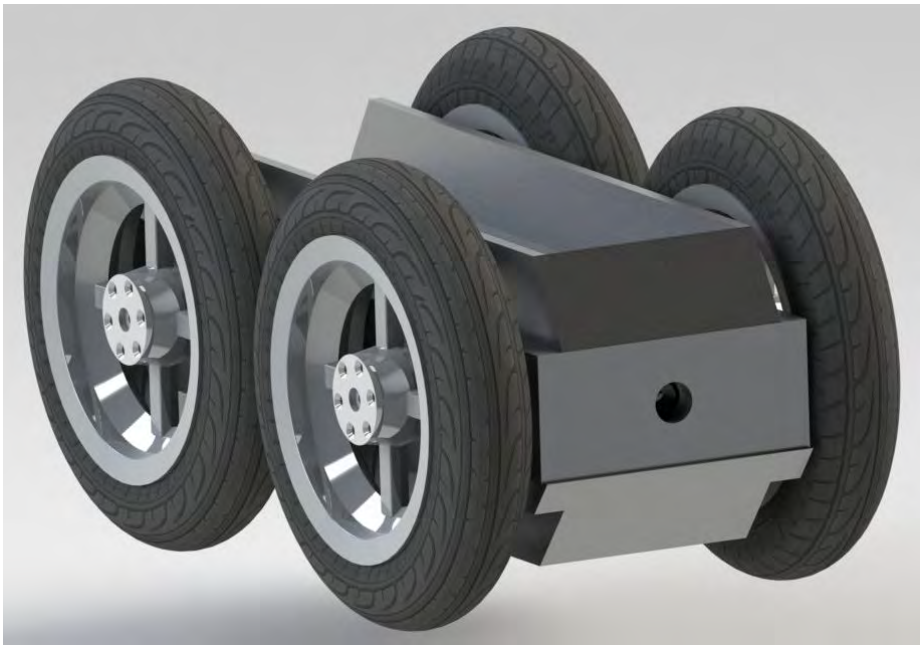

Figure 2. Robotic vehicle used in pipe inspection whose parameters were used in the simulations.

6.1 Wheel lift-off detection simulations

Two simulations were made to show the algorithm performance. In both simulations a sinusoidal voltage of 20 Vpp with 5 V offset was applied.

In the first simulation the voltage was applied with a frequency of 0.2 Hz and the vehicle was held away from the ground so that the wheels were totally free to spin without any friction force influence from the ground and the external torque profile shown in the Figure 3 was also applied.

The resulting external torque estimation is shown in Figure 4. The period between points A and B shows a positive estimation of the external torque that agrees with the actual external torque applied. The same happens from point C to point E. Between points B and C the external torque applied remains positive while the applied voltage becomes negative. In this situation the external torque is working in favor of the command, resulting in a negative estimative of the external torque. A similar case but with opposite signs can be seen between points E and F. Finally, in the last interval, both applied voltage and external torque are negative, resulting in a positive estimation of the external torque, similar to interval A through B.

ISSN 2176-5480

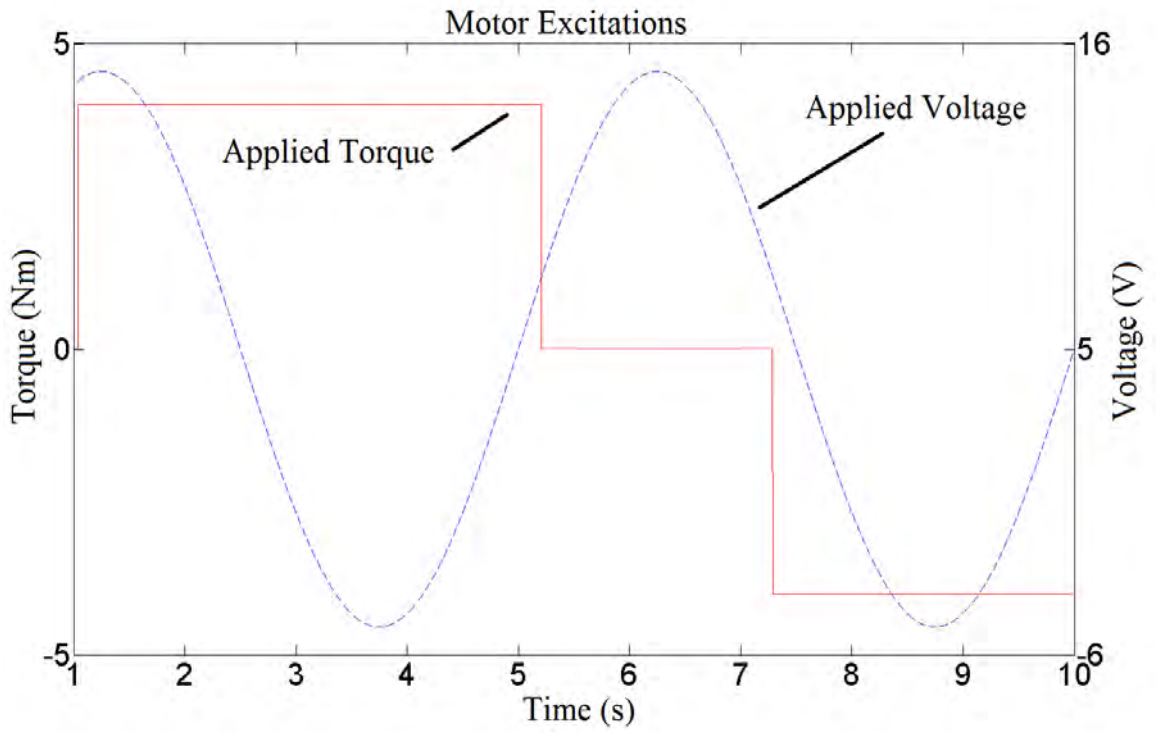

Figure 3. Applied voltage and torque upon the motor during simulation.

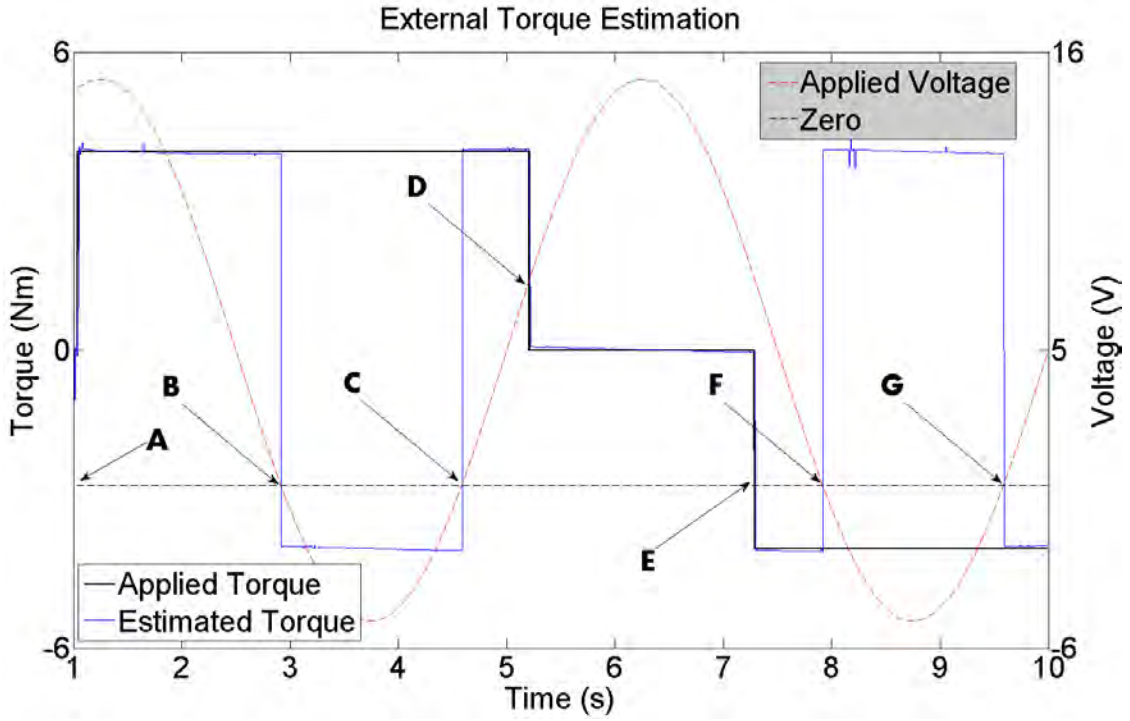

Figure 4. Comparison between applied voltage, applied torque and estimated torque from one of the vehicle wheels.

ISSN 2176-5480

In the second simulation the voltage was applied with a frequency of 0.1Hz and the vehicle was left in contact with the terrain. The friction coefficient was artificially increased to 2 so that the wheels have little or none longitudinal slip. The smoothness of the applied voltage also allowed the vehicle to accelerate with low longitudinal slip witch can be seen in the first 2 s of simulation from one of the front wheels (wheel 1) in Figure 5. This longitudinal slip solely on the front wheel happens due to the decrease of the normal force during acceleration.

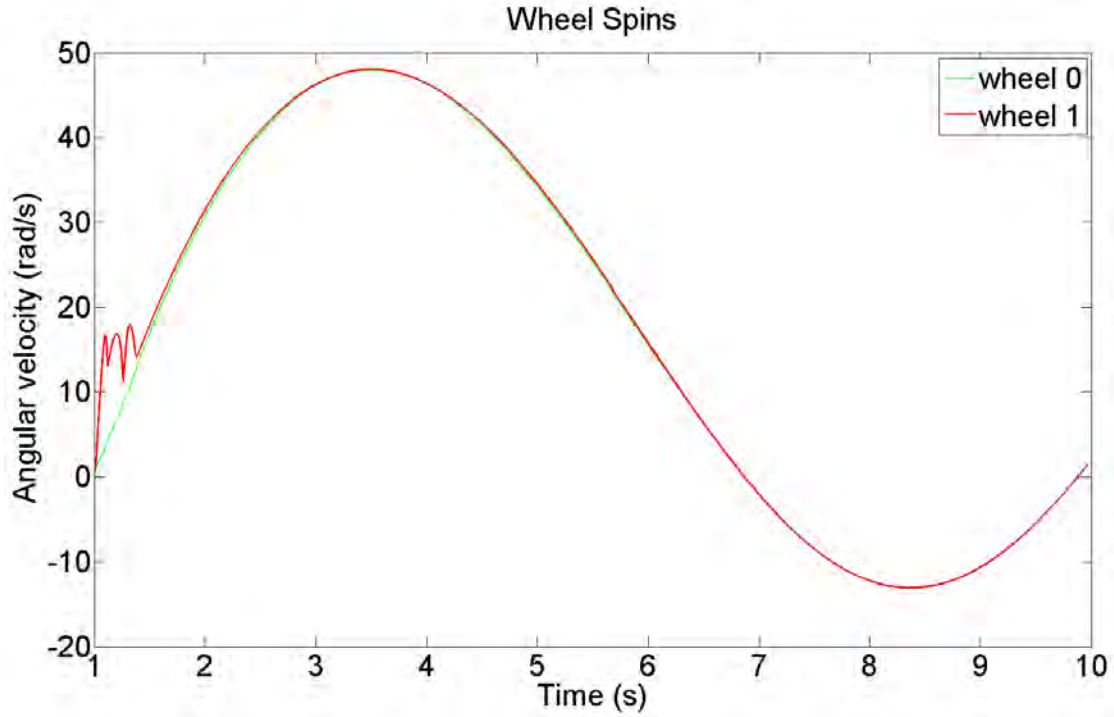

Figure 5. Angular Velocity from the right back wheel (wheel 0) and right front wheel (wheel 1).

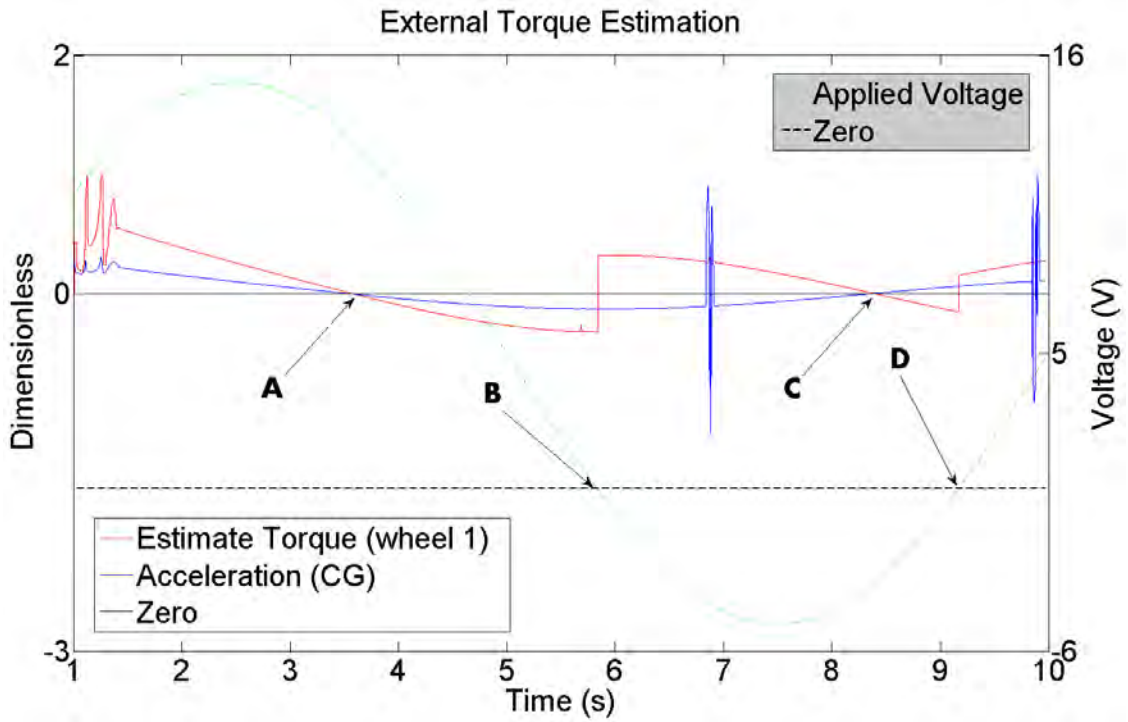

Figure 6. Comparison between applied voltage, external torque estimative and vehicle acceleration.

ISSN 2176-5480

The resulting external torque estimation is shown in Figure 6. It can be seen four important moments to be analyzed. From the simulation beginning through point A the vehicle is being accelerated. In this situation the vehicle inertia is opposing the control command represented by the applied voltage sign. From point A on, the wheel's spin is greater than the desire vehicle speed (that can be estimated by the applied voltage and motor spin) and although the applied voltage remains positive, the motor begins to work as generator, braking the vehicle. This change on how the motor is acting upon the system can be seen in the sign chance of the external torque estimative. Point B shows a change in the control command causing an instant change in the external torque estimative sign. In C the a similar situation described in point A but with opposite signs can be seen. From point D on the control command is positive again and against the inertia tendency causing an instant change in the external torque estimative.

6.2 Pitch control during ballistic motion

To test the pitch control algorithm and the lift-off wheel detection, a simulation of the vehicle hitting a 3 m high ramp was done. The ramp was modeled as a bell shaped curve (Gaussian) located at the end of the track. The vehicle was accelerated until the desired speed of 10 m/s was reached. The speed control used was a PI controller of gains Kp = 5.0 N/s and Ki = 1.0 N. The loop control frequency for the pitch control was of 20 Hz while the frequency of the torque loop control was of 1 kHz. Also, the simulator does not deal with impacts. The simulations were terminated immediately before the vehicle hit the ground so to avoid the impact.

The pitch control assumes the wheel torque command as soon as the ballistic motion is detected, overwriting the speed controller commands. Figure 7 shows the pitch angle and angular velocity of the chassis during the simulation. The simulation of the pitch control algorithm is compared with a simulation where the speed controller keeps acting on the vehicle even after the ballistic motion has begun.

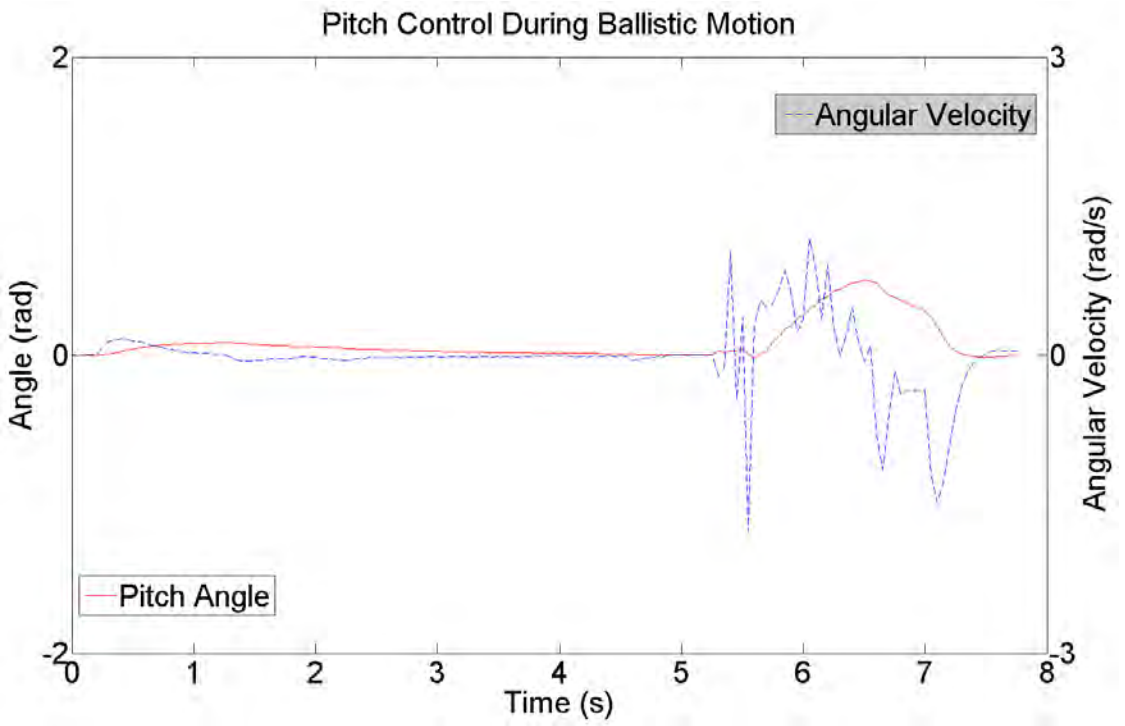

Figure 7. Pitch control of the vehicle chassis with the proposed algorithms.

Figure 8 shows the lift-off wheel detection algorithm compared to the sum of the actual normal forces. One can see in Fig. (8) that around 5.5 s the total normal forces starts to oscillate indicating that the vehicle has hit the ramp and has begun to climb it. After 7 s both the sum of normal forces and the lift-off detection algorithm are informing that the ballistic motion has begun. Simultaneously, from Fig. (7), one can see that around 5.5 s the pitch angle starts to increase indicating that the vehicle is climbing the ramp. Suddenly, around 7 s, after a brief period of constant negative angular velocity (indicating a descent), the angular velocity becomes even more negative abruptly which coincides with the ballistic motion detected in Fig. (8). Afterwards both pitch angle and angular velocity are corrected to zero and the simulation is terminated.

ISSN 2176-5480

Figure 9 shows the pitch angle and angular velocity of the vehicle chassis when no pitch control is applied but the speed controller remains acting even after detaching of all wheels from the ground. One can see that around 7 s, during ballistic motion, while trying to maintain the desired speed, the PI controller accelerates the wheels increasing the pitch angle of the vehicle. By the time that the simulation is terminated the pitch angle of the chassis is almost pi/2 rad, which is assumed to be a bad angle for landing.

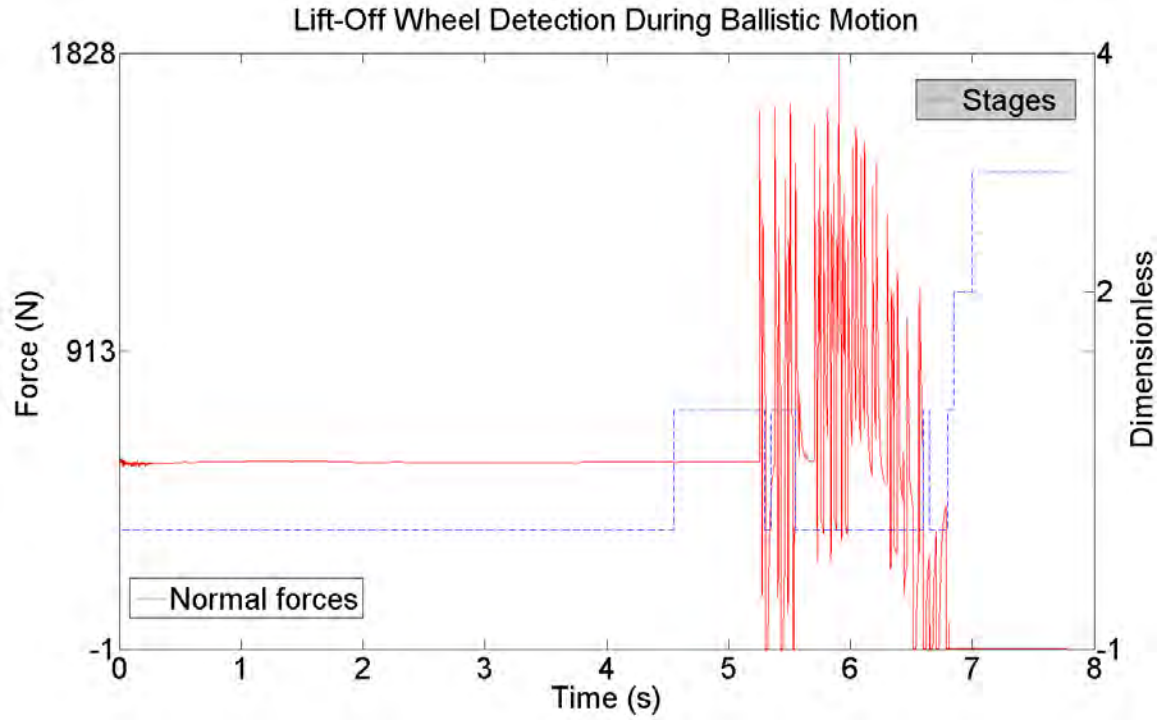

Figure 8. Comparison between the lift-off wheel detection algorithm and the sum of the actual normal forces.

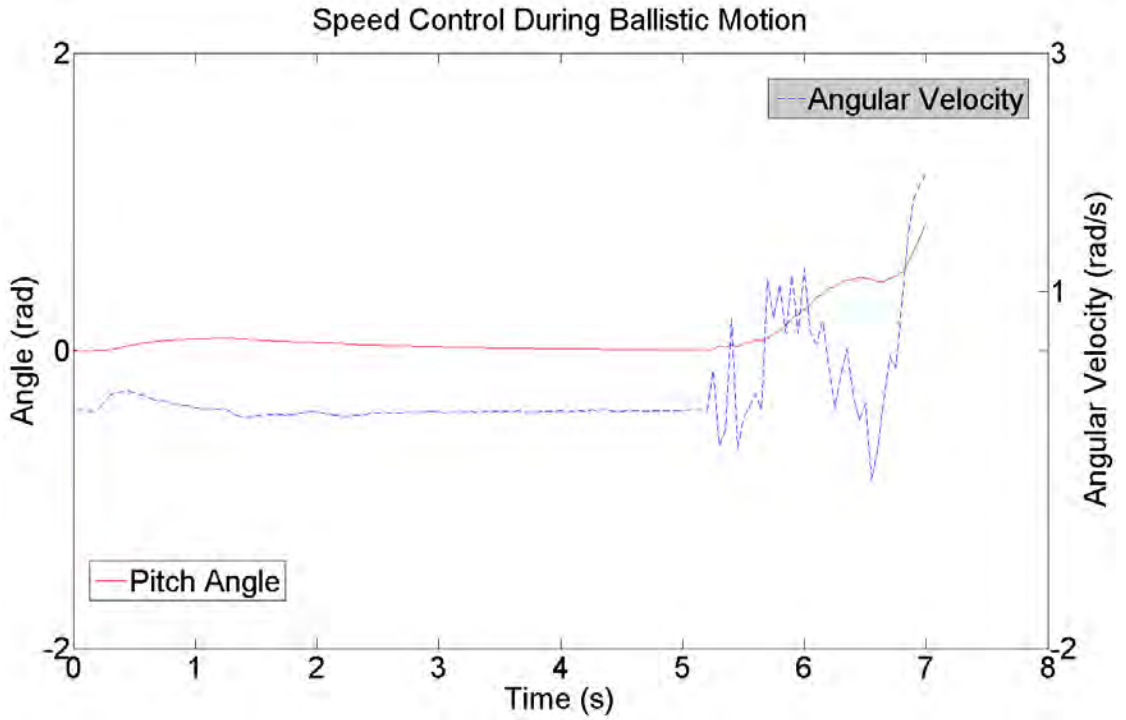

Figure 9. Pitch angle of the vehicle chassis without the proposed algorithms.

ISSN 2176-5480

7. CONCLUSIONS

This work presented a lift-off wheel detection algorithm based only in electric current sensors and encoders, which are sensors already installed on DC motors that include torque control. This costless technique can also be used to estimate external torques acting on wheels. The proposed algorithm is able not only to estimate the magnitude of the external torque, but also whether the applied torque is against the control's command or not. A four stage algorithm was proposed to shield the ballistic motion detection, as the noise of the sensors mays lead to false-positive detection of lift-off wheels. A pitch control during ballistic motion that aims to increase the odds of a safe landing was also presented. The proposed algorithm ensures that, if the initial conditions of the ballistic motion satisfy a certain relation, then the chassis of the vehicle will have its pitch angle and angular velocity equal to zero in approximate 0.3 s without saturating the motors. The algorithms were tested in a simulator developed exclusively for this research.

8. REFERENCES

Beal, Craig E. 2011. *Applications of Model Predictive Control to Vehicle Dynamics for Safety and Stability.* Department of Mechanical Engineering, Stanford University. Stanford : s.n., 2011. Tese de Doutorado.

Carlson, Christopher R. and Gerdes, J. Christian. 2003. Optimal Rollover Prevention with Steer by Wire and Differential Braking. *Proceedings of the ASME Dynamic Systems and Control Division.* November 16-21, 2003, pp. 345-354.

Genta, Giancarlo. 1997. *Motor Vehicle Dynamics: Modeling and Simulation.* Singapore : World Scientific. Publishing Co. Pte. Ltd., 1997.

Hori, Y., Toyoda, Y., Tsuruoka, Y. 1997. Traction Control of Electric Vehicle Based on Estimation of Road Surface Condition-Basic Experimental Results Using the Test EV "UOT Electric March". *Proceedings of Power Conversion Conference.* 1997, pp. 1 - 8.

Iagnemma, Karl and Dubowsky, Steven. 2004. Traction Control of Wheeled Robotic Vehicles in Rough Terrain with Application to Planetary Rovers. *The International Journal of Robotics Research.* Outubro-Novembro 2004, pp. 1029-1040.

Iagnemma, Karl, et al. 2003. Experimental Study of High-Speed Rough-Terrain Mobile Robot Models for Reactive Behaviors. *Experimental Robotics VIII.* s.l. : Springer Berlin Heidelberg, 2003, pp. 654-663.

IEA - International Energy Agency. www.iea.org. [Online] [Citado em: 23 de 05 de 2013.] http://www.iea.org/publications/globalevoutlook_2013.pdf.

Jaza, Reza N. 2009. *Vehicle Dynamics: Theory and Aplication.* New York : Springer, 2009.

Krneta, Radojka, Antic, Sanja e Stojanovic, Danilo. 2005. Recursive Least Square Method inParameters Identification of DC Motors Models. *Facta Universitatis Series: Electronics and Energetics.* 2005, pp. 467-478.

Lima, Ricardo Morrot. 2010. *Simulação Tridimensional em Tempo Real de Veículos Robóticos em Terrenos Acidentados.* Departamento de Engenharia Mecânica, PUC-Rio. 2010. Dissertação de Mestrado.

Nudehi, Shahin S., et al. 2008. Satellite Attitude Control Using Three Reaction Wheels. *American Control Conference.* 11-13 de June de 2008, pp. 4850-4855.

Ogata, Katsuhiko. 2011. *Engenharia de controle moderno.* 5ª. São Paulo : Pearson, 2011.

Peters, Steven C. 2012. *Optimal Planning and Control for Hazard Avoidance of Front-Wheel Steered Ground Vehicles.* Department of Mechanical Engineering, Massachusetts Institute of Tecnology. Boston : s.n., 2012. Tese de Doutorado.

Peters, Steven C., Frazzoli, Emilio e Iagnemma, Karl. 2011. Differential Flatness of a Front-Steered Vehicle with Tire Force Control. *International Conference on Intelligent Robots and Systems.* 2011, pp. 298-304.

Rajamani, Rajesh. 2012. *Vehicle Dynamics and Control.* New York : Springer, 2012.

Ramesh, K., et al. 2010. Design of Current Controller for Two Quadrant DC Motor Drive by Using Model Order Reduction Technique. *International Journal of Computer Science and Information Security.* 2010, pp. 17-24.

Salah, Mohammed S. Z. 2009. *Parameters Identification of a Permanent Magnet DC Motor.* Departamento de Engenharia Eleétrica, The Islamic University of Gaza. 2009. Dissertação de Mestrado.

Santos, Auderi Vicente. 2007. *Controle de Capotagem e Deslizamento de Sistemas Robóticos Móveis em Terrenos Acidentados.* Departamento de Engenharia Mecânica, PUC-Rio. Rio de Janeiro : s.n., 2007. Dissertação de Mestrado.

Santos, Ilmar Ferreira dos. 2001. *Dinâmica de Sistemas Mecânicos: Modelagem, Simulação, Visualização, Verificação.* São Paulo : Makron Books, 2001.

Schofield, Brad. 2006. *Vehicle Dynamics Control for Rollover Prevention.* Department of Automatic Control, Lund University. Lund : s.n., 2006. Tese de Doutorado.

Silva, Alexandre F. Barral, et al. 2010. A Rough Terrain Traction Control Technique for All-Wheel-Drive Mobile Robots. *Journal of the Brazilian Society of Mechanical Science & Engineering.* Outubro-Dezembro de 2010, pp. 489-501.

Silva, Alexandre Francisco Barral. 2007. *Modelagem de Sistemas Robóticos Móveis para Controle de Tração em Terrenos Acidentados.* Departamento de Engenharia Mecânica, PUC-Rio. Rio de Janeiro : s.n., 2007. Dissertação de Mestrado.

Three-axis Attitude Control with Two Reaction Wheels and Magnetic Torquer Bars. Roberts, Bryce, et al. 2004. Providence : s.n., 2004. AIAA Guidance, Navigation, and Control Conference and Exhibit.

Zaccarian, Luca. Università degli Studi di Roma: Corso de Robotica con Laboratorio. [Online] [Citado em: 28 de maio de 2013.] control.disp.uniroma2.it/zack/LabRob/DCmotors.pdf.

9. RESPONSIBILITY NOTICE

The authors are the only responsible for the printed material included in this paper.